Available online at www.sciencedirect.com
ScienceDirect
Polymer 48 (2007) 4097–4107
polymer
www.elsevier.com/locate/polymer

Broadband dielectric spectroscopy of nanostructured maleated polypropylene/polycarbonate blends prepared by *in situ* polymerization and compatibilization

Samy A. Madbouly[1], Joshua U. Otaigbe*

School of Polymers and High Performance Materials, The University of Southern Mississippi, Hattiesburg, MS 39406, United States

Received 19 February 2007; received in revised form 10 May 2007; accepted 11 May 2007
Available online 18 May 2007

Abstract

The miscibility and molecular dynamics of nanostructured maleated polypropylene (mPP)/polycarbonate (PC) blends prepared by *in situ* polymerization of macrocyclic carbonates with polypropylene modified with 0.5 wt% of maleic anhydride-reactive groups were investigated over a wide range of frequencies (10^{-2}–0.5×10^{7} Hz) at different constant temperatures using broadband dielectric spectroscopy and scanning transmission electron microscope (STEM). The molecular dynamics of the glass relaxation process of the blend (α-relaxation process) appeared at a lower temperature range compared with that of the pure PC. This shift in the molecular relaxation process is attributed to the partial miscibility of the two polymer components in the blends as previously confirmed by the morphology via STEM. Nanoscale morphologies with average domain diameters as small as 50 nm were obtained for the different blend compositions studied. The STEM photographs show that the graft mPP-*g*-PC prefers to locate at the interfaces as previously reported. The relaxation spectrum of pure PC and mPP/PC blends was resolved into α- and β-relaxation processes using the Havriliak–Negami equation and ionic conductivity. The dielectric relaxation parameters, such as relaxation peak broadness, maximum frequency, f_{max}, and dielectric strength, $\Delta\varepsilon$ (for the α- and β-relaxation processes), were found to be blend composition dependent. The kinetics of the α-relaxation processes of the blends were well described by Vogel–Fulcher–Tammann (VFT) equation. The local process of PC was resolved into two relaxation processes β_1 and β_2, associated with the carbonyl groups' motion and the combined motions of carbonyl and phenylene groups, respectively. Only β_2 shifted to lower frequency in the blend while β_1 was relatively not affected by blending. The electric modulus of the blends was used to get a sufficient resolution of the different relaxation processes in the samples, i.e., α-, β-relaxation processes, ionic conductivity, and interfacial polarization. In addition, the blending method used was found to increase the *d.c.* conductivity without affecting the charge carrier transport mechanism, making it possible to develop novel polymer blends with tunable dielectric properties and morphology from existing polymers.
Published by Elsevier Ltd.

Keywords: Molecular dynamics; Dielectric strength; Nanostructured polymer blends

1. Introduction

In the past, the inability to control phase separation and domain size precluded polymer blends from many applications due to a reduction in desired physical properties. However, better control of these problems is achieved by using block, graft or star copolymers as compatibilizing agents, but prediction and control of the structure evolution in the blends are still an elusive goal in polymer science research. These compatibilizing copolymers migrate to the phase interface, reducing surface tension and thus increase the thermodynamic stability of immiscible polymer blends [1–9]. Most compatibilizing copolymers are expensive, not available commercially, and are often difficult to synthesize. Therefore, it is essential to replace these copolymers by using an alternative and efficient method

* Corresponding author. Tel.: +1 601 266 5596.
E-mail address: joshua.otaigbe@usm.edu (J.U. Otaigbe).
[1] Present address: Cairo University, Faculty of Science, Department of Chemistry, Orman-Giza 12613, Egypt.

0032-3861/$ - see front matter Published by Elsevier Ltd.
doi:10.1016/j.polymer.2007.05.020

to produce compatible polymer blends with desired properties for a number of applications.

Relative to mechanical mixing of premade polymers, reactive blending is a cost-efficient method for producing stable nanoscale morphology with desired properties for targeted applications. In this case, the two components of the blend contain chemical reactive groups that can react together at elevated temperatures during the processing of the two polymers to produce graft copolymers. This *in situ* reactive blending can facilitate enhanced dispersion of the minor phase into smaller droplets than that of the premade copolymers. Moreover, the extent of the polymer particle size reduction is strongly dependent on the concentration of the chemical coupling agent used. This reactive blending approach has recently attracted and received attention from a number of research groups who have reported a number of successful attempts to produce a thermodynamically stable nanoscale co-continuous structure from different kinds of reactive polymer blends [10–17].

While the idea of *in situ* polymerization has been used successfully to create important commercial polymers [e.g., poly(acrylonitrile-*co*-butadiene-*co*-styrene), ABS] with improved properties, it is noteworthy that the specific approach described in this article and elsewhere [18,19] is relatively new and different from that used commercially. Like others have reported [10–17], this new approach provides a hierarchical structure, affording unparalleled polymer blend structure and property enhancement, making the approach potentially widely applicable. The *in situ* polymerization and compatibilization of this study allow for improved control of the domain size and interface, consequently yielding very small domain sizes with enhanced benefits as previously reported [18].

In the current study, the fast anionic ring-opening polymerization (ROP) of cyclic aromatic carbonate monomers in a matrix of polypropylene was used to produce a nanostructured polymer blend with unique and interesting properties [18,19]. The advantages of using anionic ROP are fast reaction kinetics, high monomer conversion, no side product, low viscosity of the oligomeric mixtures, and elimination from the polymer processing equipment of highly corrosive chemicals such as phosgene. The resulting nanostructured polymer blend is expected to contain a unique structure where one polymer is dispersed in another continuous polymer phase at molecular length scales that are impossible to achieve via classical polymer blending [18,19]. This *in situ* chemical reaction can reduce interfacial tension between the components of the polymer blend, allowing generation of large aggregates of the nano-dispersed phase particles by preventing the small particles from coalescing in the continuous polymer phase. This potential to combine, in a single material, two immiscible polymer components at the nanometer molecular length scale is thought to represent an exciting possibility with important implications for the rational design of novel multifunctional materials having a wide range of prescribed structures and properties.

To get deep fundamental insights into the macromolecular structure and functionalities, molecular dynamics, and the nature of interactions in the polymer blends of the current study, dielectric relaxation spectroscopy (DRS) was used to probe the motion of dipolar groups attached to the polymer molecular chains. DRS has been widely used in polymer relaxation analysis and has the advantage over dynamic mechanical methods in that it covers much wider frequency ranges. The use of DRS to investigate the degree of miscibility of polymer blends has been reported by several authors [20–23]. Although DRS requires that at least one of the species has a permanent dipole moment, it can also be used with advantage in blends in which one of the blend components is non-polar and thus invisible to the dielectric technique. This permits specific monitoring of the motion of the polar component as in the blend system of the present study.

In this article, the molecular dynamics of blends prepared via *in situ* polymerization and compatibilization of polycarbonate (PC) with polypropylene modified with 0.5% maleic anhydride-reactive groups is investigated using broadband DRS and scanning transmission electron microscope (STEM). The effect of the nanoscale morphologies of these blends on the kinetics of glass and local relaxation processes is examined. The different relaxation processes in the blends are analyzed using the Havriliak–Negami and ionic conductivity equations. The molecular dynamics of the glass relaxation process in the blends is also described using the Vogel–Fulcher–Tammann (VFT) equation. Finally, the electric modulus is used to describe the dielectric behavior of the blend system studied with a high degree of resolution of the different relaxation processes existing in the blends.

2. Experimental section

2.1. Materials and blend preparation

The maleic anhydride grafted polypropylene (mPP) used in this study, Polybond® 3150, was supplied by Uniroyal Chemical Crompton Corp., in the form of pellets. Its melt flow rate (230 °C/2.16 kg) was 50 g/10 min and the maleic anhydride content was 0.5 wt%. The macrocyclic carbonate with repeat units ranging from 2 to 10 was obtained from General Electric Plastics, Inc. Tetrabutylammoniumtetraphenylborate (TBATPB, obtained from Aldrich Chemical Company) with 1 wt% was used as catalyst [24–26]. All the materials were thoroughly dried in a vacuum oven overnight, prior to grinding into powders using a mortar and pestle.

Polymerization of macrocylic carbonate and blending with mPP were carried out using a Haake Minilab® counter-rotating twin-screw extruder (Rheomex CTW5). All the reactants involved in the polymerizing system were fed together into the extruder that was preheated to 225 °C and mixed for the desired mixing time. The weight-average molecular weight and polydispersity index of the pure PC obtained from the ring-opening polymerization were about 200,000 g/mol and 2, respectively [19]. The extruded PC and blends were subsequently compression molded at 220 °C for 5 min into thin films (0.1 mm thick) with no air bubbles prior to the dielectric measurements described below.

2.2. Dielectric measurements

Broadband dielectric measurements were carried out over nine decades of frequency (i.e., 10^{-2}–0.5×10^{7} Hz) at different constant temperatures using dielectric analyzer and advanced software obtained from Novocontrol™. The sample temperature was stable within less than ±0.1 K. The effective diameter of the sample was 20 mm, and the blend thickness was about 0.1 mm as already described. The dielectric measurements were carried out using two gold coated cooper electrodes with 20 mm diameter upper electrode and 30 mm diameter lower electrode. The capacitance of the condensers used in the dielectric measurements was about 30 pF.

3. Results and discussion

3.1. Molecular dynamics of pure components

A typical dielectric spectrum (dielectric permittivity, ε' and dielectric loss, ε'' versus frequency in a double logarithmic scale) for the pure PC obtained from the ring-opening polymerization process as already described at different constant temperatures is shown in Fig. 1. Clearly, this figure shows only a single peak corresponding to the α-relaxation process with almost constant dielectric strength (i.e., constant height and broadness) regardless of the different temperatures. This relaxation process is systematically shifted to higher frequency with increasing temperatures in a manner that is consistent with typical molecular dynamics of all polymer materials at temperatures higher than the T_g. This relaxation process is attributed to the micro-Brownian cooperative motions of the PC main-chain backbone that is associated with the T_g of PC. At very high frequencies (10^4–10^7 Hz), one can see a slight increase in the dielectric loss immediately after the dielectric loss peak of the α-relaxation process. This slight increase in the dielectric loss is attributed to the tail of the local process (β-relaxation process) of PC that normally appears at a very low temperature range as will be discussed later. The α-relaxation process merges with β-relaxation process to form a complex αβ-process, in which the side group rotation is cooperative with the main-chain motion. In such a complex αβ-process the two relaxation processes must be separated before the kinetics of the molecular dynamics of each process can be analyzed independently. At very low frequencies, an abrupt increase in the dielectric loss was clearly observed due to the dominant effect of the polarization by migrating charges (or ionic conductivity). The dispersion region of ε' occurs at the same frequency range (10–10^6 Hz) of the peak maximum in ε'' and shifts to higher frequency with increasing temperature. The magnitude of ε' increases with increasing temperature especially at the low frequency range due to the contribution of the ionic conductivity as already mentioned [28,29].

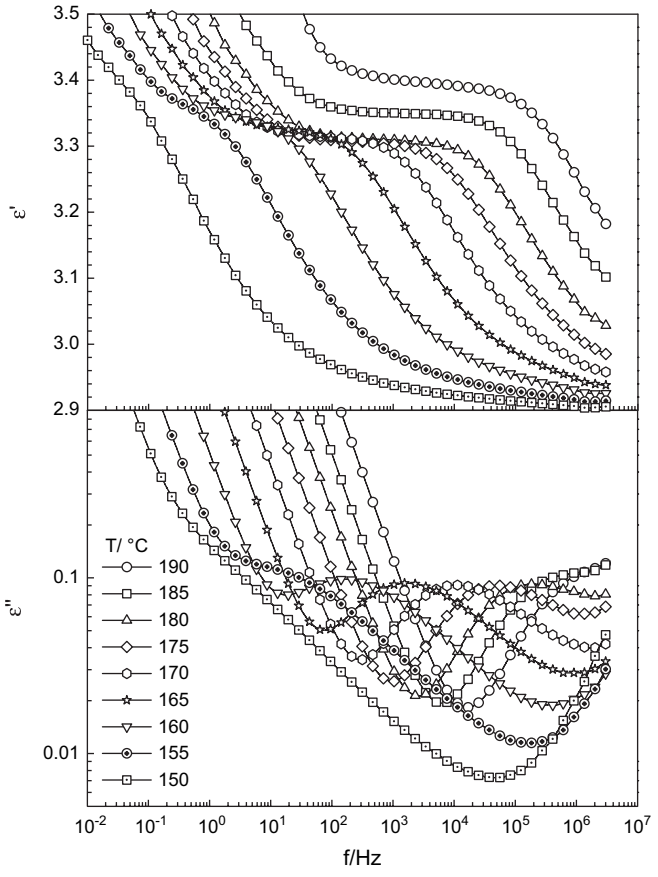

Fig. 1. Dielectric permittivity (ε') and loss (ε'') of pure PC as a function of frequency at different temperatures for the α-relaxation process.

Fig. 2 shows the dielectric spectrum of pure mPP at different temperatures. Obviously, the values of ε' and ε'' are very low compared to the corresponding values of pure PC depicted in Fig. 1. This observation is attributed to the fact that the number of re-oriented dipoles in mPP is much lower than that of PC (i.e., mPP is less polar than PC). This spectrum (Fig. 2b) appears at a very low temperature range compared to that of pure PC because the T_g of PC is much higher than that of mPP. The dielectric relaxation peak of mPP in Fig. 2b is the α-crystallization process, α_c, and is related to the various forms of imperfections that include cilia, chain loops at the lamellar surface, chain rotations and twisting within the interior of crystals, discontinuities, etc. [30–34]. This process is also related to the constrained amorphous region that exists close to the crystalline surface of mPP. The restriction of the chain motion by crystals generally leads to an apparent increase in the T_g (i.e., α-relaxation process is shifted to lower frequency). This α_c-relaxation process is temperature dependent and behaves as a typical glass relaxation process, originating from the micro-Brownian cooperative reorientation of highly constrained polymeric segments.

3.2. Molecular dynamics of blends

Figs. 3 and 4 show two examples for the dielectric spectra (dielectric permittivity, ε' and dielectric loss, ε'' versus frequency) of PC/mPP = 90/10 and 60/40 blends. One can see that, the dielectric relaxation peak of the PC-rich phase is considerably changed with blend composition (Figs. 3 and 4). The α-relaxation process is shifted to a lower temperature range

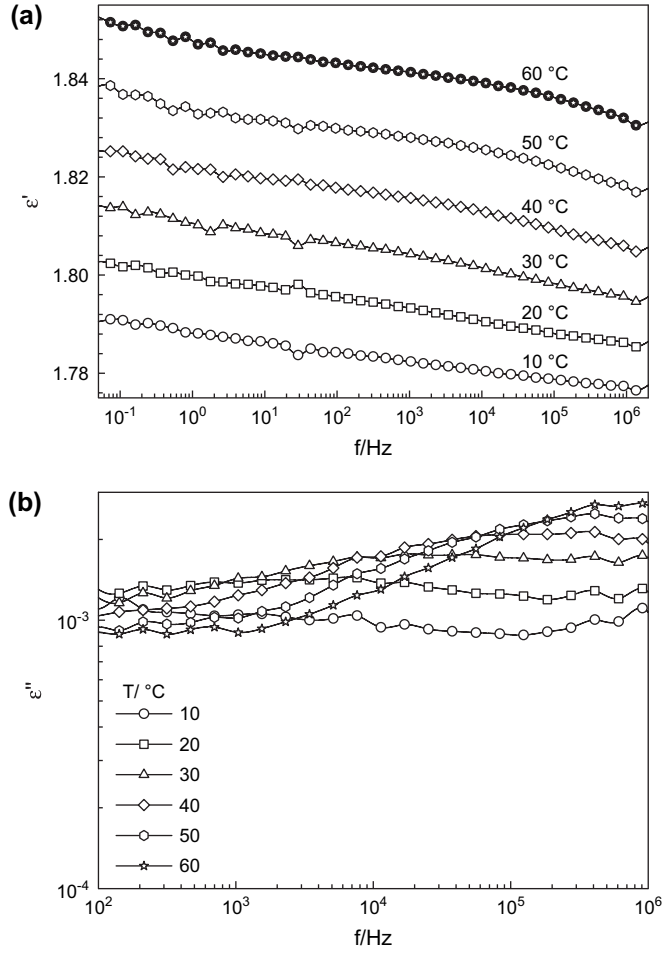

Fig. 2. (a) Dielectric permittivity (ε') of the pure mPP as a function of frequency at different temperatures. (b) Dielectric loss (ε'') of the pure mPP as a function of frequency at different temperatures.

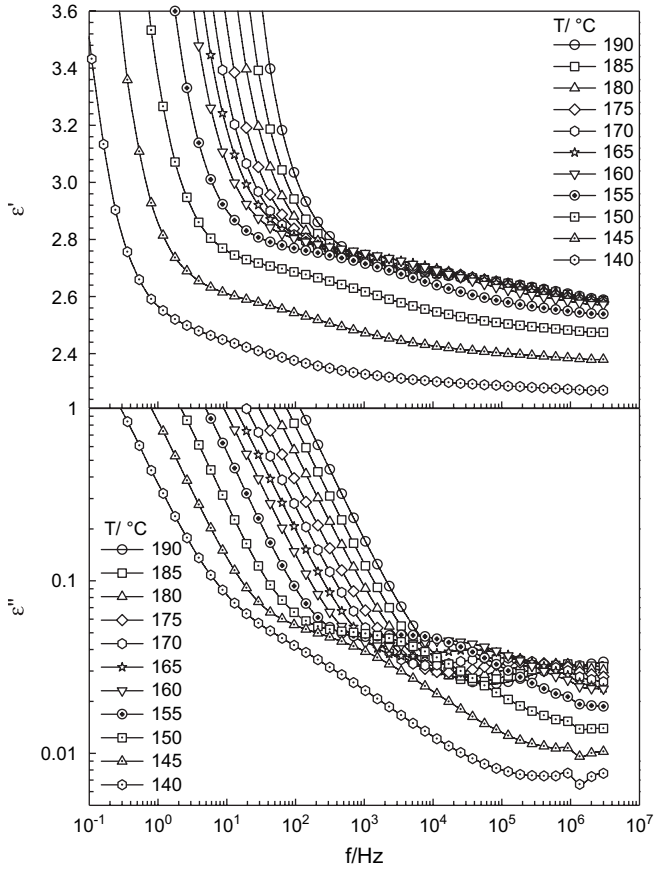

Fig. 3. Dielectric permittivity (ε') and loss (ε'') of the PC/mPP = 90/10 blend as a function of frequency at different temperatures.

and the height of the loss peak decreased with decreasing concentrations of PC in the blends. This experimental fact suggests that the *in situ* polymerization and compatibilization of PC/mPP blend produce partially miscible blends. The contribution of a very strong ionic conductivity process at low frequency ranges introduces errors in the dielectric measurements and must be subtracted from the original data for accurate data analysis as discussed later. The height of the α-relaxation process decreases with decreasing concentrations of PC due to the dilution effect of mPP. This is because the mPP is much less polar than PC as already mentioned. The dielectric spectrum of the mPP-rich phase is very low in intensity due to the low polarity of mPP and the dilution effect produced by PC. Therefore, no reliable dielectric spectra can be detected for the mPP-rich phase in these blends. The dielectric permittivity, ε' shows similar behavior. However, the dispersion region of ε' at the frequency range of the peak maximum in ε'' is not clearly observed in the ε' versus frequency plots due to the weak relaxation process of the PC-rich phase and the strong ionic conductivity in these materials.

Fig. 5 depicts the dielectric spectra (ε' and ε'' versus frequency) of different compositions of PC/mPP blends showing clear relaxation peaks at 160 °C for most of the blends. As clearly seen in this figure the maximum of the dielectric loss peak of the α-relaxation process (f_{max}) of the PC-rich phase strongly depends on the blend composition. For example, the f_{max} of PC/mPP = 90/10 blend is about two decades higher than that of pure PC. Similar shift in f_{max} (i.e., two decades higher than that of pure PC) was observed for PC/mPP = 10/90 blend. However, the f_{max} of PC/mPP = 60/40 blend shifts to higher frequency by only one decade compared to the f_{max} of pure PC. This experimental finding indicates that the partial miscibility of the blend components in PC/mPP blends is high when the concentration of PC is either very high (90 wt%) or very small (10 wt%) as shown in Fig. 5. The frequency dependence of ε' showed similar behavior with very high conductivity of the blends compared to that of the pure PC.

In a previous paper the morphology of the current polymer system was investigated as a function of composition using scanning transmission electron microscopy (STEM) [18]. The STEM [27] image for mPP/PC = 90/10 blend after extrusion showed black PC dispersions encased within the mPP matrix as previously reported [18]. The diameters of the PC domains were measured using an image analysis software (ImageJ™)[18]. Elliptical nanoscale morphology of PC with an average diameter of 150 ± 5 nm was observed as previously

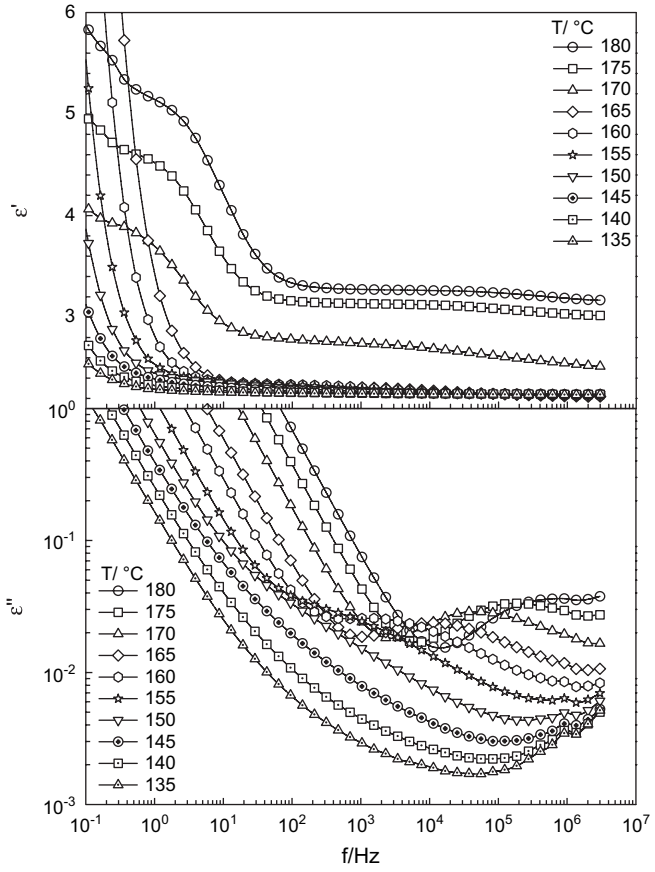

Fig. 4. Dielectric permittivity (ε') and loss (ε'') of the PC/mPP = 60/40 blend as a function of frequency at different temperatures.

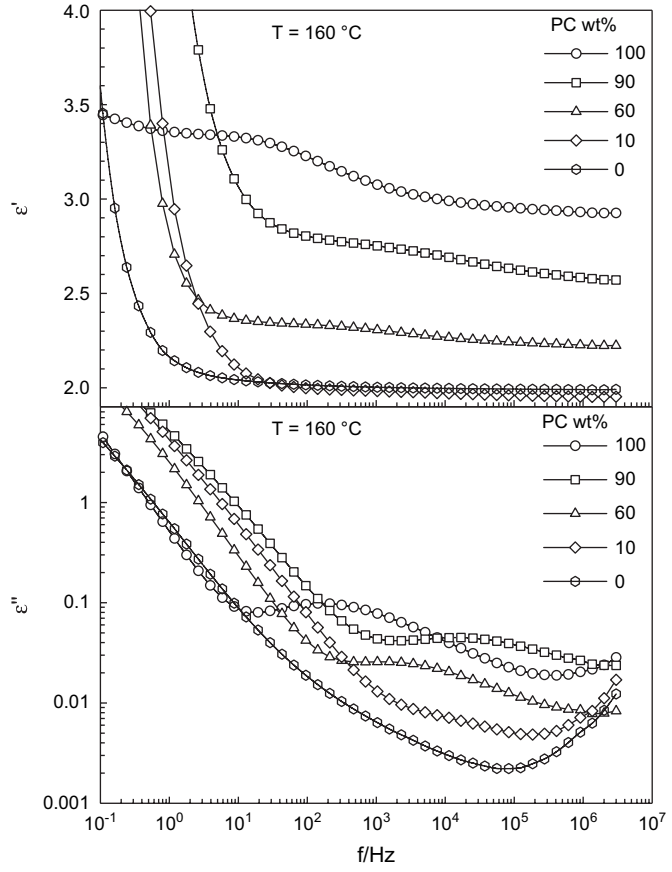

Fig. 5. Dielectric permittivity (ε') and loss (ε'') as a function of frequency for different blend compositions at 160 °C.

reported [18]. The ellipsoidal PC morphology was attributed to the formation of micelles of the grafted block copolymer (PC-*g*-PP) that was produced during the *in situ* polymerization and compatibilization [18]. In addition, nanoscale morphology with an average domain size as small as 50 nm was obtained for the mPP/PC = 10/90 blend at identical extruder rotation speed and temperature (rpm = 200 and $T = 225$ °C) used in the current study [18]. This composition showed a very fine mPP dispersion in PC matrix which is typically related to the micelles of graft copolymers produced during the polymerization and compatibilization reactions [18]. The STEM photograph also confirmed that the graft PC-*g*-PP prefers to locate at the interfaces. Based on the above morphological observations it appears that the shift of f_{max} to higher frequency (lower temperature) of the blends is related to the nanoscale morphologies of the blends and the high possibility of formation a graft copolymer during the *in situ* polymerization and compatibilization of the blend in the batch mixer. This conclusion is consistent with the hypothesis that the *in situ* polymerization and compatibilization of this blend induced formation of a partially miscible blend particularly at high shear rate during the processing condition of the batch mixer.

The relaxation time τ can be calculated from the analysis of dielectric spectra based on Eq. (2) as discussed in the next section. The values of τ as a function of the reciprocal temperature for the α-relaxation processes of the blends of the PC-rich phase are shown in Fig. 6. These curves are useful for judging the partial miscibility of the blends. Clearly, the activation energy curve of PC/mPP = 90/10 blend shifted to lower temperatures compared with that of pure PC, indicating that some amount of mPP is dissolved in the PC-rich phase.

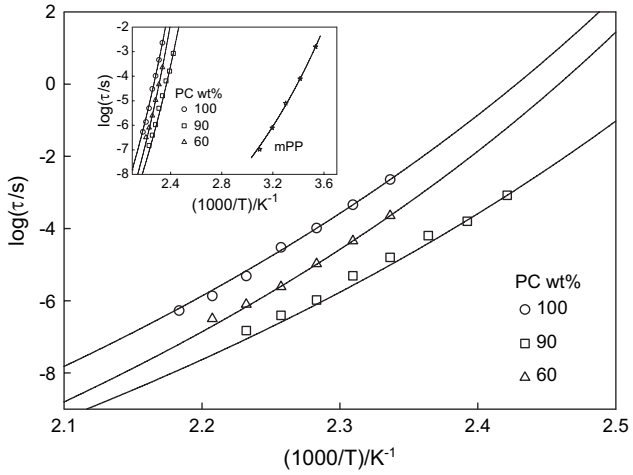

Fig. 6. Relaxation times as a function of reciprocal temperature for different blend compositions. The solid lines show the fitting to the VFT equation. The inset-plot shows the same figure plus the activation energy curve of pure mPP.

The activation energy curve of PC/mPP = 60/40 blend also shifts to lower temperature but to a lesser extent compared to that of PC/mPP = 90/10 blend, indicating that the amount of mPP dissolved in PC-rich phase for the PC/mPP = 90/10 blend is higher than that of the PC/mPP = 60/40 blend under identical processing conditions. However, both of the blends just mentioned are partially miscible blends with both of them containing small amounts of mPP dissolved in PC-rich phase. Note that the inset-plot of Fig. 6 shows the activation energy curves of these three samples plus that of pure mPP. Obviously, the activation energy curve of pure mPP is located at very low temperature ranges and the shifts of the activation energy curves of the blends to lower temperature ranges are very small, supporting our assumption that the amount of mPP dissolved in the PC-rich phase is very small. This partial miscibility behavior is supported by DSC measurements previously reported elsewhere (i.e., the T_g of the PC-rich phase in the blends is shifted to lower temperatures) [18].

3.3. Theoretical analysis of experimental data

It is widely accepted that the relaxation process connected to the onset of large-scale micro-Brownian cooperative motion above T_g in polymers can be interpreted by Vogel–Fulcher–Tammann (VFT) equation [35]:

$$\tau = \tau_0 \exp\left[\frac{B}{T - T_0}\right] \tag{1}$$

where τ and T are, respectively, relaxation time and temperature; τ_0, B and T_0 are fitting parameters with different physical significance. The symbols in Fig. 6 are experimental data while the lines are fitting lines using non-linear regression technique. Clearly, Fig. 6 shows a good description of the data by using VFT equation and Table 1 shows the fitting parameters obtained from this analysis.

In the analysis of the dielectric spectra of PC and blends (Figs. 1, 3 and 4), it is necessary to separate the strong contribution of the ionic conductivity and local relaxation process from the main relaxation process (α-relaxation). The dielectric relaxation spectra of the blends can be resolved into three processes, α-, β-relaxation processes, and ionic conductivity. The α- and β-relaxation processes can be simulated using the following Havriliak–Negami (HN) equation [36]:

Table 1
Fitting parameters of the VFT equation to the experimental data

PC/wt%	τ/s	T_0/K	B/K
100	2.1×10^{-13}	400	1300
90	4×10^{-13}	395	1100
60	7×10^{-13}	390	1010
10	5×10^{-13}	387	1001
0	2×10^{-13}	220	950

$$\varepsilon^* = \varepsilon_\infty + \frac{\varepsilon_0 - \varepsilon_\infty}{\left[1 + (i\omega\tau)^b\right]^c} \tag{2}$$

where ω is the angular frequency ($\omega = 2\pi f$); b and c are parameters that describe the shape of the relaxation time distribution function; τ is the relaxation time and ε^* is the complex dielectric permittivity. When $c = 1$, the above equation reduces to the Cole–Cole relationship (symmetrical curves) [37]. The contribution of the ionic conductivity to the measured dielectric loss can be described by:

$$\varepsilon'' = \frac{\sigma_{dc}}{\varepsilon_0 \omega} \tag{3}$$

where σ_{dc} is the *d.c.* conductivity. The dielectric relaxation parameters (i.e., relaxation strength, $\Delta\varepsilon$, maximum relaxation frequency, f_{max}, and distribution parameters of each process) can be obtained from this analysis. The circular symbols in Fig. 7a and b (for pure PC and PC/mPP = 60/40 blend, respectively) represent the experimental data, while the dotted lines represent the contribution of each relaxation process according to the HN equation [36]. The solid line passing through the experimental points is the total sum of the three processes. Clearly, a good description of the experimental data was obtained as shown in Fig. 7.

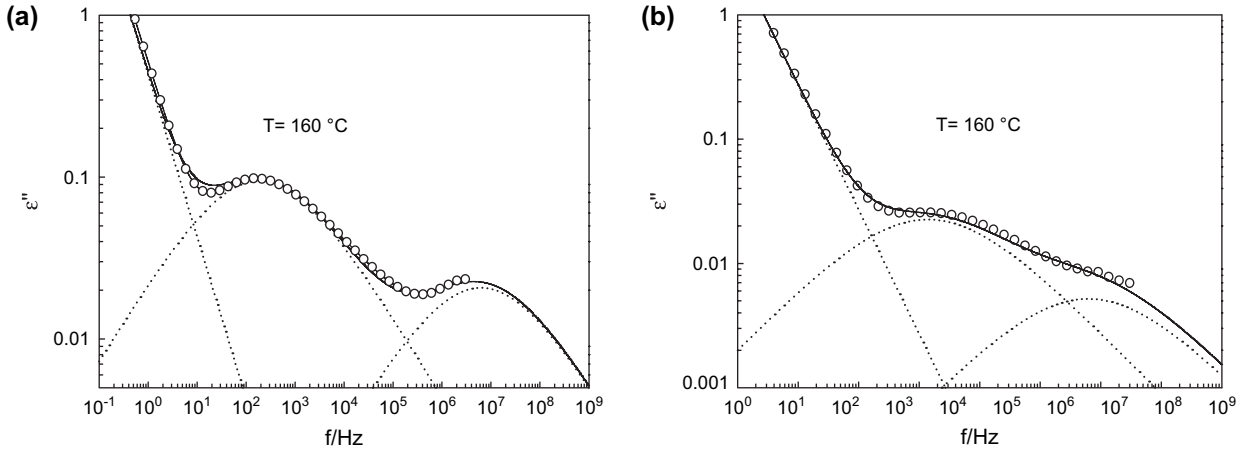

Fig. 7. Fits of HN Eq. (2) to the dielectric spectrum of: (a) pure PC at 160 °C and (b) PC/mPP = 60/40 blend at 160 °C.

The composition dependence of the dielectric strengths of the α- and β-relaxation processes, $\Delta\varepsilon_\alpha$ and $\Delta\varepsilon_\beta$, respectively, is shown in Fig. 8. One can see that, both $\Delta\varepsilon_\alpha$ and $\Delta\varepsilon_\beta$ decrease strongly with decreasing concentrations of PC in the blends. The decrease is very sharp when the concentration of PC > 60 wt%. At lower concentrations the values of $\Delta\varepsilon_\alpha$ and $\Delta\varepsilon_\beta$ decrease very slightly with decreasing concentration of PC. Based on this experimental fact, it appears that the formation of partially miscible blends and/or graft copolymer of PC-*g*-PP decreases both the side group rotations and the main-chain motions, leading to subsequent decrease of $\Delta\varepsilon_\beta$ and $\Delta\varepsilon_\alpha$, respectively. Fig. 8 also supports the formation of PC-*g*-PP copolymer during the *in situ* polymerization and compatibilization because the incorporation of non-polar chains of PP to the main chains of PC led to a dramatic decrease in the dielectric relaxation strengths of both α- and β-relaxation processes as shown in the figure. If these blends are immiscible or even partially miscible, the decrease of $\Delta\varepsilon_\alpha$ and $\Delta\varepsilon_\beta$ with composition should be linear or show slightly negative deviation from the linear-mixing rule. However, in the present mPP/PC blend system both $\Delta\varepsilon_\alpha$ and $\Delta\varepsilon_\beta$ reached 20% of its original strength when the concentration of mPP is only 40%.

The $\Delta\varepsilon$ at a given temperature can be obtained according to the following Frohlich–Onsager equation [38–40]:

$$\Delta\varepsilon = \varepsilon_0 - \varepsilon_\infty \propto \frac{n}{T} g(T)\mu^2(T) \tag{4}$$

where n is the number density of dipole moments, g is the orientation correlation factor and μ is the dipole moment. This approximation gives $\Delta\varepsilon$ that is proportional to the number of dipole moments at a given temperature. The observed decrease in the value of $\Delta\varepsilon_\alpha$ and $\Delta\varepsilon_\beta$ can be attributed to the partial miscibility of the two polymer components.

The formation of graft copolymer of PC-*g*-PP and the partial miscibility of the blend would also influence the dynamical constraints of polymer chain relaxation motions. It is well established that the dynamical constraints can be studied by monitoring the change in the distribution of relaxation times (peak width) of the specific process under consideration [20–23,41,42]. The greater the variation in the dynamical constraints, the broader the relaxation process. Fig. 9 shows the normalized curves for the α-relaxation process for different blend compositions after subtraction of the ionic conductivity and β-relaxation process based on the above analysis using Eqs. (2) and (3). One can see in Fig. 9 that the *in situ* polymerization and compatibilization led to a considerable change in the width of the relaxation spectra. This broadening in the dielectric spectrum can be attributed to different environments, which would lead to a variation in the consistency of the cooperative regions and in turn produce a greater variation in the dynamical constraints of segments as a result of blending.

3.4. Molecular dynamics of the local relaxation process

The β-relaxation process is believed to be correlated with the mechanical properties of the blends such as ductility, impact strength and toughening. Studies of the blend dynamics of the β-relaxation process are of considerable practical interest and have received much attention. The secondary relaxation of polycarbonate and other related engineering thermoplastics has been extensively investigated over the past decades [43–50]. At a very low temperature range (−110 to 10 °C), the local relaxation process (β-relaxation) of PC can be seen clearly as shown in Fig. 10. With increasing temperature, the loss peak maximum shifts to a higher frequency while the peak intensity slightly increases. The dispersion region of ε' occurs at the same frequency range of the peak maximum in ε'' shifting to higher frequency with increasing temperatures. Similar behavior has been detected for PC/mPP = 90/10 blends as shown in Fig. 11. It is well established in the literature that the local relaxation process mainly depends on the molecular interactions, configuration and chain packing. For example, Madbouly and Mansour investigated the molecular dynamics of the local process of tetramethyl polycarbonate (TMPC) [41,42]. The β-relaxation peak of TMPC was found to occur at 150 °C higher than that of pure PC at the same frequency range. This large difference in the temperature range of the β-relaxation process of TMPC and PC is attributed to

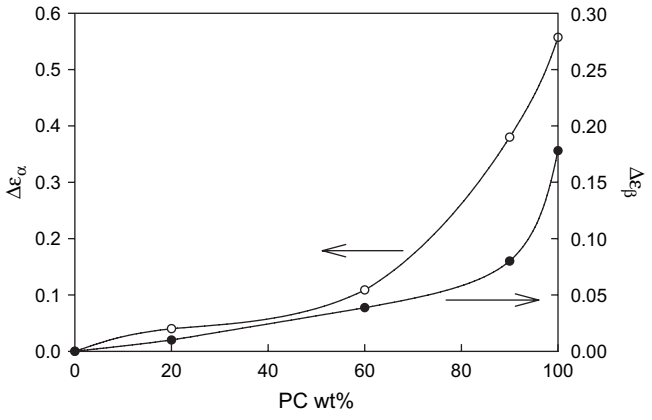

Fig. 8. Dielectric relaxation strength, $\Delta\varepsilon$ of the α- and β-relaxation processes as a function of composition.

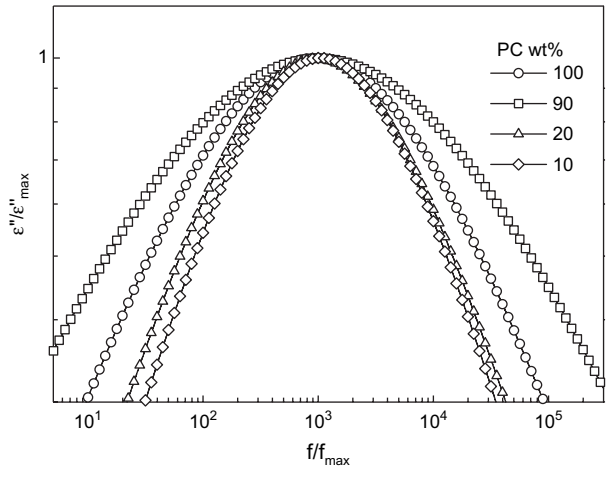

Fig. 9. Normalized dielectric spectra as a function of composition for the α-relaxation process at 160 °C.

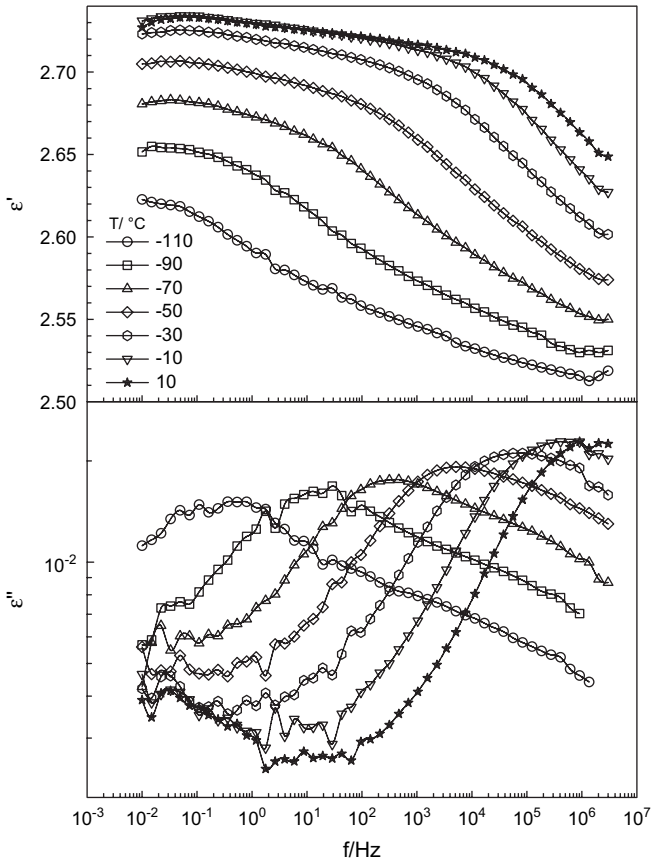

Fig. 10. Dielectric permittivity (ε') and loss (ε'') of pure PC as a function of frequency at different temperatures for the β-relaxation process.

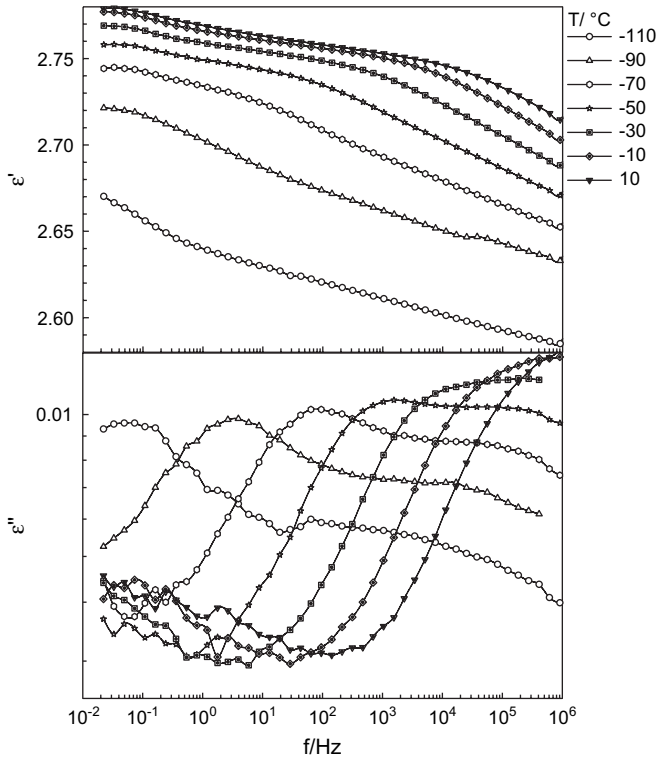

Fig. 11. Dielectric permittivity (ε') and loss (ε'') of 90 wt% PC blend as a function of frequency at different temperatures for the β-relaxation process.

the tetramethyl substitution of the phenyl rings in TMPC. In addition, it is believed that the local relaxation process is directly related to the excellent mechanical properties of PC [43–45]. The molecular dynamics of the current PC prepared from the ring-opening polymerization of macrocyclic carbonates is in good agreement with that reported in the literature [46–49].

The DRS has been used to investigate a series of poly(ester carbonate) [50]. It was concluded that there are two main contributions to the dielectric β-relaxation of PC, one assigned to the libration of the carbonyl group alone and the other to the combined motion of carbonyl and phenylene groups [50]. The local motion of carbonyl group produces a relaxation process that normally appears at low temperature or high frequency. However, the local relaxation process of the combined motion of carbonyl and phenylene groups appears at relatively higher temperature or lower frequency range compared to that of carbonyl group alone. For clarity, in the present study the local relaxation processes of the carbonyl groups and that of the combined motion of carbonyl and phenylene groups will be denoted as β_1 and β_2, respectively. Fig. 12 shows a comparison of the local relaxation spectra of pure PC and PC/mPP = 90/10 blend at −80 °C. Clearly, there are two relaxation peaks associated with the β_1 and β_2 that appear at high and low frequencies, respectively, for the two samples. The intensity of the β_2-relaxation process is much higher than that of the β_1-relaxation process, especially for the pure PC. It is clear that the strength of the two relaxation processes (β_1 and β_2) decreases significantly in the blend but the magnitude of the depression in β_2 process is much higher than that of β_1 process. In addition, the peak maximum of the β_1-relaxation process is almost the same in the blend as in pure PC. However, the peak maximum of the β_2-relaxation process is considerably shifted to lower frequency in the blend compared to that of the pure PC. This finding can be considered as an evidence for the formation of graft PC-*g*-PP during the

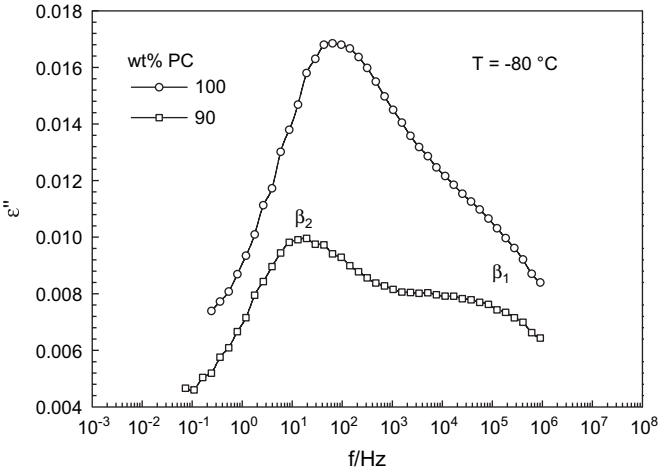

Fig. 12. Comparison of dielectric loss (ε'') as a function of frequency for pure PC and PC/mPP = 90/10 blend at −80 °C.

in situ polymerization and compatibilization process of this system, since the formation of graft copolymer can produce steric hindrance to the phenylene groups' motions. It is noteworthy that the analysis of the dielectric data of Fig. 7a and b was carried out at very high temperatures and we detected only the tail of the local process. Therefore, it is impossible to observe the two separate local relaxation processes (β_1 and β_2) at this high temperature range. These two separate local relaxation processes can also be associated with essentially the same dipole process and are a direct consequence of the correlation function controlling the reorientation of the dipole like others have reported for other polymers. For example, Williams [51] observed two sub-glass relaxations for liquid–crystalline side-chain polymers. The lower temperature one shows a small activation enthalpy (5–6 kcal mol^{-1}), and is attributed to slightly hindered internal rotations in the side group. The higher-temperature sub-glass relaxation, on the other hand, shows a higher activation enthalpy (23 kcal mol^{-1}) and a low positive activation entropy, and is attributed to restricted internal rotations of the side groups around bonds near the main chain, eventually in cooperation with the movements of the main-chain segments.

3.5. Molecular dynamics of the ionic conductivity

It is well established that the contribution of ionic conductivity to the main relaxation behavior of a polymer sample can be totally suppressed by using the complex electric modulus (M^*) developed by Macedo et al. [52].

$$M^* = \frac{1}{\varepsilon^*} = M' + iM'' = \frac{\varepsilon'}{\varepsilon'^2 + \varepsilon''^2} + i\frac{\varepsilon''}{\varepsilon'^2 + \varepsilon''^2} \tag{5}$$

Based on this equation the dielectric data can be represented as $M'(\omega)$ and $M''(\omega)$ instead of $\varepsilon'(\omega)$ and $\varepsilon''(\omega)$, respectively. Figs. 13 and 14 show the dielectric spectra of pure PC and PC/mPP = 90/10 blend as two examples for the frequency dependence of $M''(\omega)$ as a function of different temperatures. For pure PC, two separate relaxation peaks can be easily seen in Fig. 13. The first relaxation peak observed in the low frequency range (0.01–100 Hz) is attributed to the contribution of ionic conductivity to the dielectric measurements. This peak shifts to lower frequency with decreasing temperature. At high frequency range (10^2–10^6 Hz), the α-relaxation process of PC is clearly shown to be totally resolved from the contribution of ionic conductivity. Similar behavior was observed for PC/mPP = 90/10 blend (Fig. 14), i.e., the ionic conductivity is totally separated from the α-relaxation process of PC-rich phase. At a very low frequency range (0.01–1 Hz) another relaxation peak can be clearly seen. This peak is related to some accumulation of charge carriers at the interface of mPP dispersed particle and PC matrix. This peak which is commonly called Maxwell–Wagner–Sillars (MWS) interfacial polarization peak is slightly shifted to higher frequency with increasing temperature. This peak was observed for all the present blends of different compositions in this study.

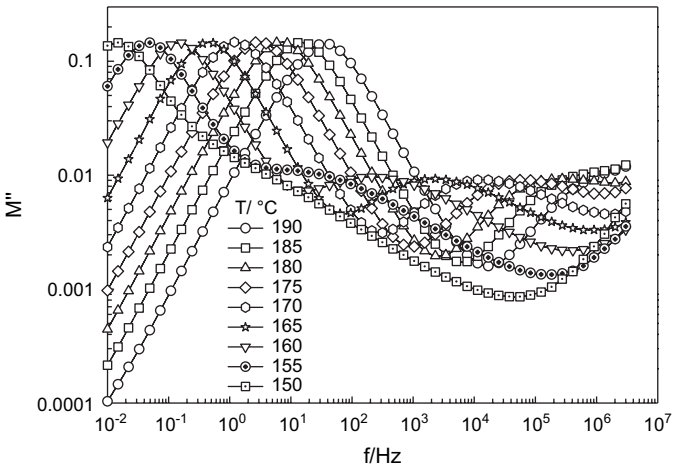

Fig. 13. Electric modulus, M'' of pure PC as a function of frequency at different temperatures.

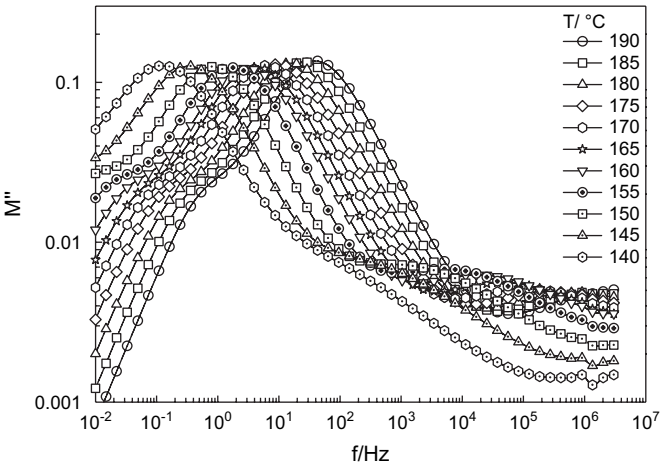

Fig. 14. Electric modulus, M'' of PC/mPP = 90/10 blend as a function of frequency at different temperatures.

The temperature dependence of the conductivity relaxation process obtained from the electric modulus can be described linearly using Arrhenius equation:

$$f_{mM''} = f_0 \exp\left(\frac{E_{aM''}}{kT}\right) \tag{6}$$

where $f_{mM''}$ is the frequency of the peak maximum of the conductivity relaxation process, f_0 is a material constant, k is the Boltzmann constant and $E_{aM''}$ is the activation energy. As Fig. 15 shows the activation energy curves of the conductivity relaxation processes for different blend compositions can be well described by the Arrhenius equation. This finding suggests that the charge carrier transport mechanism was unaffected by blending. The activation energy decreased from 3.25 eV for pure PC to 1.796 eV and to 2.083 eV for PC/mPP = 90/10 and 60/40 blends, respectively. Therefore, the rate of conductivity increased in the blends compared to that of the pure PC due to the fact that the T_g of mPP is much lower than that of pure PC. It must be stated here that there is no general trend for the temperature dependence of the ionic

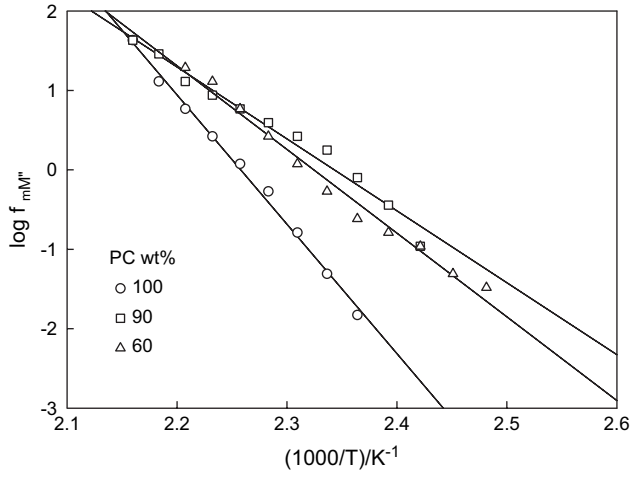

Fig. 15. Arrhenius plots of the temperature dependence of the conductivity peak maxima ($f_{m_M''}$) for different blend compositions.

conductivity; for some polymers, such as, polyurethane (PU), the charge carrier transport mechanism is governed by the cooperative motion of polymer chain segment (i.e., follow the VFT equation) [52]. For some other polymers, such as, poly(styrene-*co*-acrylonitrile) (SAN) and poly(2-hydoxyethyl methacrylate) (PHEMA), the temperature dependence of ionic conductivity follows Arrhenius equation as in the current system described in this article [53,54].

4. Conclusions

It can be concluded from the results of this study that the molecular dynamics of the pure PC exhibited two processes, β- and α-relaxation processes located at low and high temperature ranges, respectively. A very weak relaxation process (α_c-relaxation process) is observed for pure mPP which is attributed to the constrained amorphous region existing close to the crystalline surface of mPP. The molecular dynamics of the α-relaxation process was changed strongly by blending, i.e., the dielectric spectrum of the PC/mPP blend appears at lower temperatures compared to that of the pure PC, indicating that mPP is partially miscible with PC. The kinetics of α-relaxation process of the pure components and PC/mPP blends were well described by VFT equation. The dielectric spectra of the pure PC and blends were analyzed based on Havriliak–Negami and ionic conductivity equations. The composition dependence of the dielectric strength of α- and β-relaxation processes ($\Delta\varepsilon_\alpha$ and $\Delta\varepsilon_\beta$, respectively) showed a very large negative deviation from the linear-mixing rule. This is thought to be related to the formation of graft copolymer of PC-*g*-PP. The dielectric data were well represented by the electric modulus to get a sufficient resolution of the different relaxation processes in the samples, i.e., α-, β-relaxation processes, ionic conductivity, and interfacial polarization. In addition, we have found that the *in situ* polymerization and compatibilization process of this system produced more steric hindrance to the local relaxation process of the phenylene group motions. The charge carrier transport mechanism was not changed by blending, i.e., the mechanism was well described by Arrhenius equation regardless of the blend composition. The *d.c.* conductivity of the blend increased significantly due to the presence of mPP (low T_g component). This study may stimulate a better understanding of the dynamics and transport mechanisms in the little studied nanostructured polymer blend systems, making an important contribution to the literature on molecular dynamics of polymers and to the alternative paradigm of exploiting the hierarchical nanostructured polymer blend functionalities, rather than the intrinsic physical properties of the blend components to yield novel nanoscale morphology and properties.

Acknowledgments

This work was primarily supported by the Division of Chemical and Transport Systems Program of the U.S. National Science Foundation under Award Number CTS-0317646. We thank Dr. Brunelle for providing us with the macrocylic carbonates and Dr. Mauritz Research Group for providing us with direct access to their Broadband dielectric spectrometer, and for assistance with raw data acquisition. The anonymous reviewer is thanked for bringing to our attention the work of Graham Williams.

References

[1] Wilkinson AN, Ryan AJ. Polymer processing: structure development. Dordrecht, The Netherlands: Kluwer; 1998.
[2] Shull KR, Kramer EJ. Macromolecules 1990;23:4769.
[3] Fredrickson GH, Bates FS. J Polym Sci Part B Polym Phys 1995; 35:2775.
[4] Washburn NR, Lodge TP, Bates FS. J Phys Chem 2000;B104:6987.
[5] Fredrickson GH, Bates FS. Eur Phys J 1998;B1:71.
[6] Hillmyer MA, Maurer WW, Lodge TP, Bates FS, Almdal K. J Phys Chem 1999;B103:4814.
[7] Hamley IW. The physics of copolymers. New York: Oxford University Press; 1998.
[8] Binder K. Advances in polymer science series, vol. 138. Berlin: Springer; 1999.
[9] Macosko CW. Macromolecules 1996;29:5590.
[10] Ryan AJ. Nat Mater 2002;1:8.
[11] Ruzette AV, Leibler L. Nat Mater 2005;4:19.
[12] Pernot H, Baumert M, Court F, Leibler L. Nat Mater 2002;1:54.
[13] Kietzke T, Nether D, Landfester K, Montenegro R, Guentner R, Scherf U. Nat Mater 2003;2:408.
[14] Pan L, Chiba T, Inoue T. Polymer 2001;42:8825.
[15] Jafari SH, Peotschke P, Stephan M, Warth H, Albert H. Polymer 2002;43:6985.
[16] Pan L, Inoue T, Hayami H, Nishikawa S. Polymer 2002;43:337.
[17] Pamell S, Min K. Polym Eng Sci 2005;45:876.
[18] Madbouly SA, Otaigbe JU, Ougizawa T. Macromol Chem Phys 2006;207:1233–43.
[19] Alam TM, Otaigbe J, Rhoades D, Holland GP, Cherry BR, Kotula PG. Polymer 2005;46:12468–79.
[20] Zidan HM, Tawansi A, Abu-Elnader M. Physica B Condens Matter 2003;339:78.
[21] Yiwen A, Jerry S. J Polym Sci Part B Polym Phys 2003;41:927.
[22] Zhang S, Painter PC, Runt J. Macromolecules 2002;35:8478.
[23] Fukao K, Uno S, Miyamoto Y, Hoshino A, Miyaji H. Phys Rev E Stat Nonlin Soft Matter Phys 2001;64:051807/1.
[24] Brunelle DJ, Evans TL, Shannon TG, Boden EP, Stewart KR, Fontana LP, et al. Polym Prepr (Am Chem Soc Div Polym Chem) 1989;30:56.

[25] Brunelle DJ. Trends Polym Sci 1995;3:154.
[26] Brunelle DJ, Shannon TG. Macromolecules 1991;24:3035.
[27] Müller SA, Goldie KN, Bürki R, Häring R, Engel A. Ultramicroscopy 1992;46:317.
[28] Kyritsis A, Oissis P, Grammatikakis J. J Polym Sci Polym Phys 1995; 33:1737.
[29] Mitzner E, Goering H, Becker R. Angew Makromol Chem 1994; 220:177.
[30] Ishida Y, Watanabe M, Yamafuji K. Kolloid Z 1964;200:48.
[31] Peterlin A, Holbrook JD. Kolloid Z 1965;203:68.
[32] Sasabe H, Saito S, Asahina M, Kakutani H. J Polym Sci Polym Phys 1969;7:1405.
[33] Nakagawa K, Ishida Y. J Polym Sci Polym Phys 1973;11:1503.
[34] Karasawa N, Goddard III WA. Macromolecules 1995;28:6765.
[35] Ferry JD. Viscoelastic properties of polymer. New York: Wiley; 1980.
[36] Havriliak S, Negami S. Polymer 1967;8:161.
[37] Cole RH, Cole KS. J Chem Phys 1941;9:341.
[38] Boettcher CIF, Van Belle OC, Rip A. Theory of dielectric polarization I. Amsterdam: Elsevier Scientific; 1973.
[39] McCrum NG, Read BE, Williams G. Anelastic and dielectric effects in polymeric solids. Dover Publishers; 1991.
[40] Diaz-Calleja R, Riande E, San Roman J. Macromolecules 1991;24:264.
[41] Mansour AA, Madbouly SA. Polym Int 1995;36:269.
[42] Mansour AA, Madbouly SA. Polym Int 1995;37:267.
[43] Soles CL, Douglas JF, Jones RL, Wu W. Macromolecules 2004;37:2901.
[44] Soles CL, Douglas JF, Wu W, Peng H, Gidley DW. Macromolecules 2004;37:2890.
[45] Cangialosi D, Wubbenhorst M, Schutt H, van Veen A, Piquen SJ. J Chem Phys 2005;122:64702.
[46] Mansour AA, Madbouly SA, Hoehne WH. Polym Int 1996;41:395.
[47] Wuebbenhorst M, Van Koten EM, Jansen JC, Mijs W, Van Turnhout J. Macromol Rapid Commun 1997;18:139.
[48] Spall S, Goodwin AA, Zipper MD, Simon GP. J Polym Sci Part B Polym Phys 1996;34:2419.
[49] Katana G, Kremer F, Fischer EW. Macromolecules 1993;26:3075.
[50] Merenga AS, Papadakis CM, Kremer F, Liu J, Yee AF. Macromolecules 2001;34:76.
[51] Williams G. Polymer 1994;35:5170.
[52] Macedo PB, Moynihan CT, Bose R. Phys Chem Glasses 1972;13:171.
[53] Kanapitsas A, Pissis P, Estrella AG. Eur Polym J 1999;35:923.
[54] Mohomed K, Gerasimov TG, Moussy F, Harmon JP. Polymer 2005; 46:3847.